Arch. Mech., 50, 3, pp. 467–482, Warszawa 1998
FIFTY YEARS OF THE ARCHIVES OF MECHANICS

Dynamics of quantum vortices in superfluid ^{4}He

Dedicated to Prof. Henryk Zorski
on the occasion of his 70-th birthday

T. LIPNIACKI (WARSZAWA)

THE DISSIPATIVE motion of quantized vortex line, after reconnection, is studied within the localized induction approximation. The numerical simulations of vortex line evolution help to determine the rate of the line-length changes. In the absence of counterflow, the vortex line shortens after each reconnection and line-length reduction is calculated as a function of friction parameter α and reconnection angle φ. The obtained results sugest that the decay of quantized vortex tangle is due to line-length reduction which occurs after each reconnection of vortex lines. In the presence of the counterflow, however, the reconnection may initiate a generation of a cascade of vortex loops. These loops blow up, so the total length of vortices grows up and the quantum turbulence can be generated.

1. Introduction

THE LANDAU'S two-fluid theory [1] is the basis of our understanding of the peculiar flow properties of ^{4}He below the λ-point. Acording to this theory, He II (superfluid ^{4}He) is a sum of the Bose condensate (superfluid component) and the gas of thermal excitation (normal component). The rotationless flow of the superfluid component is violated on one-dimensional singularities called quantum vortices (Fig. 1), (FEYNMAN [3], ONSAGER [2]). The circulation of the superfluid

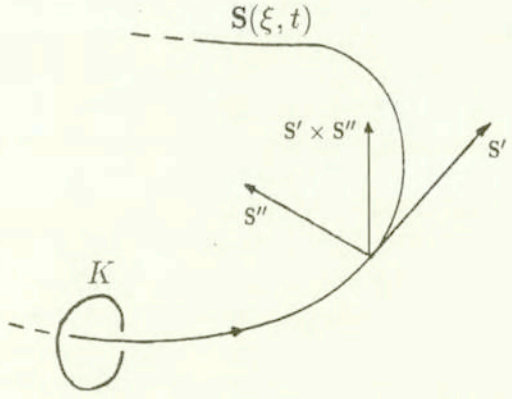

FIG. 1. Vortex line with a triad of vectors characterizing the instantaneous local configuration of the curve $s(\xi, t)$.

velocity about these lines remains constant, $\kappa = h/m_{\mathrm{He}} = 9.97 * 10^{-4}\mathrm{cm}^2/\mathrm{s}$, where h is Planck's constant, and m_{He} is the mass of helium atom. The curve traced out by a vortex filament may be specified in the parametric form $s(\xi, t)$ with t and ξ denoting time and arc length, respectively. Then the instantaneous velocity of a given point of the filament in the localized induction approximation is

$$\dot{s} = \beta s' \times s'' + V_s + \alpha s' \times (V_{ns} - \beta s' \times s'') - \alpha' s' \times [s' \times (V_{ns} - \beta s' \times s'')], \tag{1.1}$$

where prime denotes instantaneous derivative with respect to ξ, α and α' are temperature-dependent parameters which measure the frictional force exerted by the normal fluid on the vortex line. $V_{ns} = V_n - V_s$ is the difference between normal and superfluid velocities, and

$$\beta = \frac{\kappa}{4\pi} \ln\left(\frac{c}{a_0 \langle s'' \rangle}\right) \approx \kappa, \tag{1.2}$$

where κ is the quantum of circulation, c is a constant of order one, $\langle s'' \rangle$ is the average curvature of the vortices in the tangle and $a_0 \simeq 1.3 * 10^{-8}$ cm is the effective core radius of a quantized vortex. Although β has the logarithmic dependence on the tangle density since $\langle s'' \rangle$ increases as the tangle density increases, it is usually treated as a constant. The localized induction aproximation, which describes vortex motion in a much simpler way than the Biot–Savart law, is well justified when the local curvature is big enough that term $\beta s' \times s''$ is greater than the velocity induced by other vortices, or original vortex segments. Here we will base on the localized induction aproximation because of its numerical simplicity.

When the magnitude of relative velocity (counterflow) $V_{ns} = |V_n - V_s|$ becomes sufficiently large, superfluid laminar flow transforms into superfluid turbulent flow in which the quantum vortices form chaotic tangle.

The pioneerning studies of superfluid turbulence were conducted by VINEN [4], who proposed the mechanisms of vortex generation and decay. He observed that in the presence of the counterflow velocity V_{ns}, the vortex ring can blow up, and that line-line reconnections (predicted by Feynman) can give rise to new rings. Since then considerable progress has been made and the new methodology based on careful analysis of the motion of quantized vortices using extensive numerical simulation has been developed.

SCHWARZ simulated [6] the evolution of a vortex tangle basing on Eq. (1.1) describing vortex motion in the localized induction approximation, and on the assumption that vortex lines reconnect when they get close enough. Although the obtained results are in general agreement with observation, the problem is not yet sufficiently understood. The vortex tangle is characterized by its line-length density L and anisotropy coefficients. Knowing those coefficients, one can calculate the rate of vortex density growth or decay (Vinen equation). Schwarz has

found those quantities for various α (friction parameter) as the result of numerical simulations, and so has deduced the coefficients in the Vinen equation. It is still interesting to calculate the growth and decay rates in a "simpler" way – without time-consuming simulations of the whole vortex tangle.

The most important process which governs the vortex tangle evolution is the line-line reconnection (Fig. 2). Schwarz simulations confirm the observation that the density of vortex tangle depends dramatically on the assumed reconnection probability. To see why the reconnections play a crucial role in quantum turbulence, let us consider the simple evolution of a single circular vortex ring.

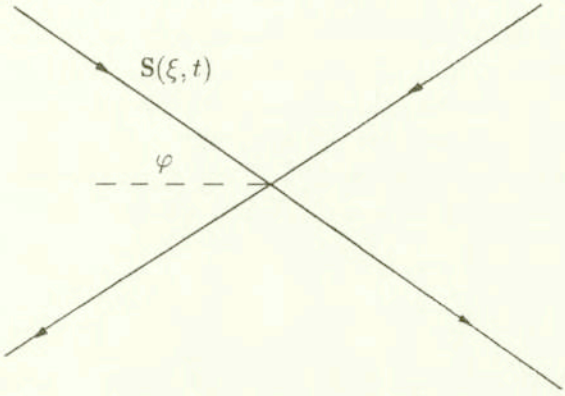

FIG. 2. Line-line reconnection configuration.

According to Eq. (1.1) we have:

$$\frac{dR}{dt} = -\frac{\alpha\beta}{R} + \alpha V_{ns}\cos\Theta\,, \tag{1.3}$$

$$\frac{d\Theta}{dt} = -\frac{\alpha V_{ns}}{R}\sin\Theta\,, \tag{1.4}$$

where R is the vortex ring radius and Θ is the angle between V_{ns} and normal to the surface containing the vortex ring. Dividing (1.3) by (1.4) and multiplying the resulting equation by $\sin\Theta$, one gets:

$$\frac{dR}{d\Theta}\sin\Theta = -R\cos\Theta + \frac{\beta}{V_{ns}}\,, \tag{1.5}$$

$$\frac{d(R\sin\Theta)}{d\Theta} = \frac{\beta}{V_{ns}}\,, \tag{1.6}$$

$$R = \frac{\beta\Theta + C}{V_{ns}\sin\Theta}\,. \tag{1.7}$$

The line $R = \beta\Theta/(V_{ns}\sin\Theta)$ in (Θ, R)-plane starting at the singular point ($R = \beta/V_{ns}$, $\Theta = 0$) separates the solutions in which R tends to infinity, from the

solutions in which R tends to zero. Namely, if

$$R > R_0(\Theta) = \frac{\beta\Theta}{V_{ns}\sin\Theta}, \tag{1.8}$$

the ring will blow up and die on the boundaries, and if $R < R_0(\Theta)$, the ring will contract to a point. The picture is not very different when instead of rings, one considers ovals. This simple example shows that to sustain turbulence, the reconnections are needed to produce new kinks which can develop into new loops (arc segments).

The aim of this paper is to consider the vortex evolution after an idealized reconnection, in the absence and in the presence of the counterflow V_{ns}. In the first case we calculate the line-length reduction resulting from a single reconnection as a function of friction coeficient α and reconnenction angle φ.

The analysis of Eq. (1.1) can be done in two steps (Schwarz). First, the factor β is absorbed into reduced time and velocity scales $\tau = \beta t$, $v = V/\beta$ to yield

$$\frac{\partial s}{\partial \tau} = s' \times s'' + v_s + \alpha s' \times (v_{ns} - s' \times s'') - \alpha' s' \times [s' \times (v_{ns} - s' \times s'')]. \tag{1.9}$$

Second, this equation is invariant under the transformation in which spatial dimensions are multiplied by a scale factor λ, time by λ^2, and velocities by λ^{-1}. If a vortex line evolution subject to the same particular velocities v_s, v_n is $s(\xi, \tau)$, then

$$s^\star(\lambda\xi, \lambda^2\tau) = \lambda s(\xi, \tau) \tag{1.10}$$

is the solution appropriate to the imposed velocities v_s/λ, v_n/λ. It means that, if all coordinates are magnified by a factor λ, and all applied velocities divided by λ, then the vortex motion will look the same, except that the time of the process increases by the factor of λ^2.

The instantaneous fractional rate of change of the line length at some particular point on a vortex is equal to $s' \cdot \dot{s}' = (s' \cdot v_s)' - \dot{s} \cdot s''$. Consequently, a given element of length $\Delta\xi$ obeys the law (SCHWARZ [6])

$$\frac{1}{\Delta\xi}\frac{\partial \Delta\xi}{\partial \tau} = \alpha[v_{ns} \cdot (s' \times s'') - |s' \times s''|^2] - \alpha' v_{ns} \cdot s'', \tag{1.11}$$

provided v_s is constant in space. As a result, line-length of vortex filament $l = \int d\xi$ satisfies the equation

$$\frac{\partial l}{\partial \tau} = \int [v_{ns} \cdot (\alpha s' \times s'' - \alpha' s'') - \alpha |s''|^2]\, d\xi. \tag{1.12}$$

2. Line evolution after reconnection

For the sake of simplicity we consider the reconnection problem of two infinite straight vortex filaments (Fig. 2). After reconnection two angles are formed. We analyse the evolution of a vortex line formed at the initial state ($\tau = 0$) angle 2φ. In fact the dynamical equation (1.1) can be used after a small time interval when the characteristic radius of curvature at the vortex vertex becomes larger than the radius of vortex core which is of the order 1–2 Å. To study the reconnection event on a macroscopic scale (1 Å) one has to use equations which model the vortex core (eg. Ginzburg–Landau) – but such a problem is far from being solved.

2.1. The case $V_{ns} = 0$

With $v_n = v_s = 0$ Eqs. (1.9), (1.12) simplyfy to

$$\frac{\partial s}{\partial \tau} = (1 - \alpha')\, s' \times s'' + \alpha s'', \tag{2.1}$$

$$\frac{\partial l}{\partial \tau} = \alpha \int |s''|^2 \, d\xi \,. \tag{2.2}$$

According to our previous considerations, Eq. (2.1) is invariant under the transformation (1.10). Since the initial conditions are also invariant under that transformation, the vortex configurations for times τ and $\lambda^2\tau$ will be similar, with similarity scale λ. In other words, the vortex line for all times will have a similar shape, whose spatial scale D is growing as $\sqrt{\tau}$. It leads to the result

$$\Delta l = A\,\tau^{1/2}, \qquad \int |s''|^2 \, d\xi = \frac{A}{2\alpha}\,\tau^{-1/2}, \tag{2.3}$$

where Δl is the line reduction and $A = A(\alpha, \alpha', \varphi)$.

The numerical simulations where performed for various angles φ, and for 5 sets of (α, α') $[(0.01, 0.005), (0.03, 0.0125), (0.1, 0.016), (0.3, 0.010), (1, -0.270)]$ corresponding to 5 different temperatures from 1.07 K° to 2.15 K°. (See also SCHWARZ [5], where line-line and line-boundary reconnections are considered.) Also the dependence of line-length reduction on parameter α' (with $\alpha = 1$) has been examined. The vortex line evolution for $\varphi = \pi/4$ and $\alpha = 0.1$ is shown in Fig. 3, the subsequent plots correspond to the vortex position at $\tau = \tau_0 i^2$ where τ_0 is arbitrary time constant and $i = 0, ..., 7$. Figure 4 shows the vortex shapes for $\varphi = \pi/6$ and two various α: 0.01 and 1. One can see that for smaller α the vortex line is more wavy.

The simulations revealed that for realistic values of $\alpha \leq 1$, $|\alpha'| < 1$, with surprising accuracy, (see Fig. 5)

Δl – does not depend of α' (to within the accuracy of 1%) (*)

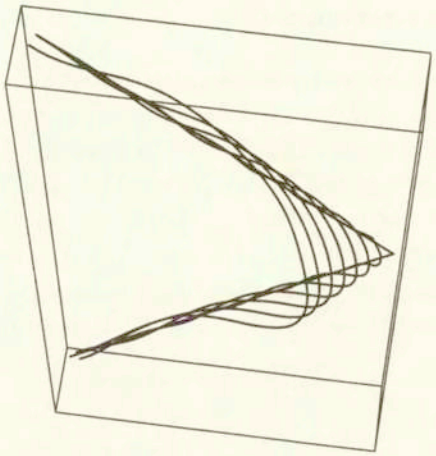

FIG. 3. Vortex line evolution after reconnection for reconnection angle $\varphi = \pi/4$, and friction coefficients $\alpha = 0.1$, $\alpha' = 0.016$. The line positions are shown at $\tau = i^2\tau_0$.

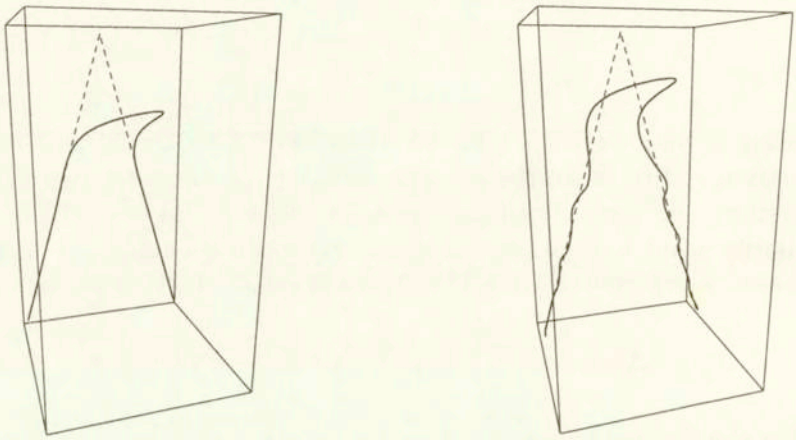

FIG. 4. The shape of vortex line for reconnection angle $\varphi = \pi/6$ and two various friction coefficients α; left – $\alpha = 1$, right – $\alpha = 0.01$. The smaller is α, the more wavy will be the vortex line.

and

$$A = B(\varphi)\,\alpha^{1/2}, \qquad \Delta l = B(\varphi)\,(\alpha\tau)^{1/2}. \tag{2.4}$$

The relations (2.4) are a simple consequence of observation (*); If line-length reduction does not depend on α' one can put $\alpha' = 1$, then the vortex evolution equation (2.1) simplifies to

$$\frac{\partial s}{\partial(\alpha\tau)} = s''. \tag{2.5}$$

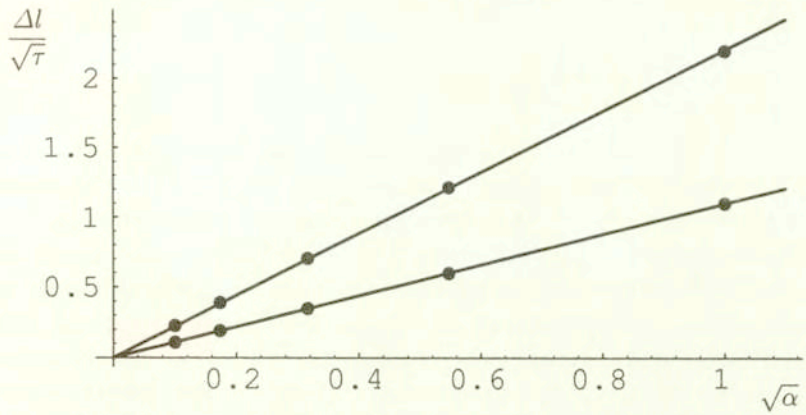

FIG. 5. $A = \Delta l/\sqrt{\tau}$ as a function of $\sqrt{\alpha}$ for two reconnection angles: $\varphi = \pi/6$ – upper line and $\varphi = \pi/4$ – lower line.

For such an evolution equation spatial dimension D and the line-length reduction Δl are proportional to $\sqrt{\alpha\tau}$.

The observation (*) and relation (2.4) can be justified as follows. Let us approximate the vortex line by the set of circular vortex segments. The line-length of the circular vortex satisfies the equation

$$\frac{\partial l}{\partial \tau} = \frac{2\pi\alpha}{R} \tag{2.6}$$

and is independent of α'. It suggests that the rate of line reduction of the whole vortex is approximately independent of α'. Moreover let us notice that for $\alpha = 0$, the vortex evolution equation (2.1) reduces to the nondissipative one,

$$\frac{\partial s}{\partial \tau} = (1 - \alpha')\, s' \times s''. \tag{2.7}$$

During the evolution governed by Eq. (2.7), the following quantities are constant in time:

$$l = \text{const}\,, \qquad \int |s''|^2 d\xi = \text{const}. \tag{2.8}$$

The first fact is the consequence of Eq. (1.8), and the second one can be proved as follows: from Eq. (2.7) one obtains

$$\dot{s}'' = s'' \times s''' + s' \times s'''' \,, \tag{2.9}$$

where the dot denotes now the instantaneous derivative with respect to $\tau^\star = (1 - \alpha')\,\tau$. Now

$$\frac{\partial}{\partial \tau^\star} \int |s''|^2 = 2 \int s'' \cdot \dot{s}'' = 2 \int s'' \cdot (s' \times s''''), \tag{2.10}$$

$$\int s'' \cdot (s' \times s'''') = \int s'' \cdot (s' \times s''')' = -\int s''' \cdot (s' \times s'''), \tag{2.11}$$

provided that

$$s'' \cdot (s' \times s''')\Big|_1^2 = 0. \tag{2.12}$$

Now, one can evaluate the vortex line step by step using the method of fractional steps. In the first half of time step we solve Eq. (2.7), in the second one we solve Eq. (2.5) using the previous result as an initial condition. The evolution governed by nondissipative Eq. (2.7) does not change the line length and does not change the squared curvature – which determine the rate of line-length changes (see Eq. (2.2)) during the evolution under Eq. (2.5). Roughly speaking, although the first term in Eq. (2.1) significantly changes the evolution of the vortex (line shape), it does not significantly influence the rate of the line-length reduction.

If we want to calculate only the length reduction, the simplified Eq. (2.5) can be used which is much simpler because the vortex line remains on a plane. Also numerically Eq. (2.5) is much more stable than Eq. (2.1), so the simulations can go faster.

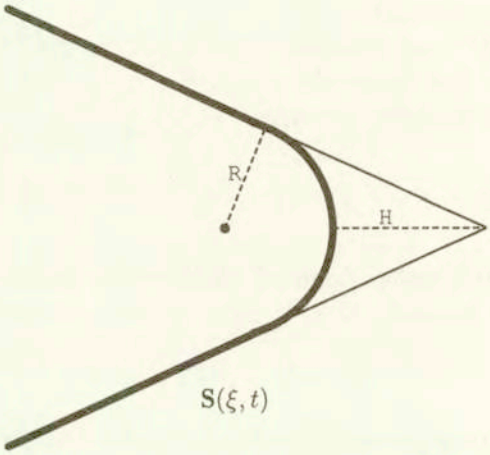

FIG. 6. The vortex line is approximated by the circle arc *plus* two semi-straight lines to calculate the rate of line reduction.

Therefore, function $B(\varphi)$, and the line-length reduction, can be estimated as follows; let us approximate the vortex line by the sum: a part of a circle tangent to the initial angle arms plus the rest of the angle (Fig. 6). As a result, we get a relation between the distance H and the radius of curvature R.

$$R = \frac{H \sin(\varphi)}{1 - \sin(\varphi)}, \tag{2.13}$$

and from Eq. (2.5)

$$\frac{\partial H}{\partial \tau} = \frac{\alpha}{R}. \tag{2.14}$$

After some algebra one gets

$$H(\tau) = \left[\frac{2\tau\alpha(1-\sin(\varphi))}{\sin(\varphi)}\right]^{1/2} \tag{2.15}$$

and

$$\Delta l = (\alpha\tau)^{1/2} B(\varphi), \tag{2.16}$$

with

$$B(\varphi) = \left[\frac{8\sin(\varphi)}{1-\sin(\varphi)}\right]^{1/2} \left(\mathrm{ctg}(\varphi) + \varphi - \frac{\pi}{2}\right). \tag{2.17}$$

Figure 7 compares the above relation with the numerical results obtained for Eq. (2.1).

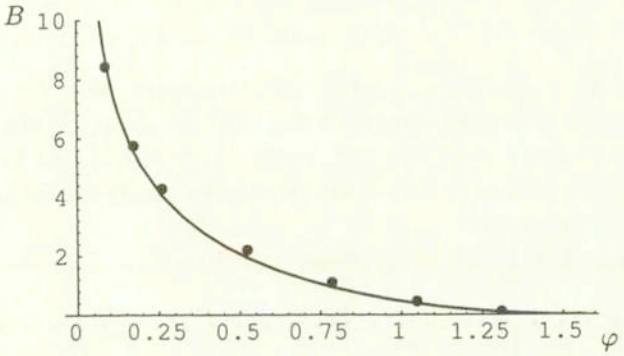

FIG. 7. Value of $B(\varphi)$ approximated by relation (2.17) (line) and calculated in numerical simulations (dots) (line reduction $\Delta l = B(\varphi)\sqrt{\alpha\tau}$).

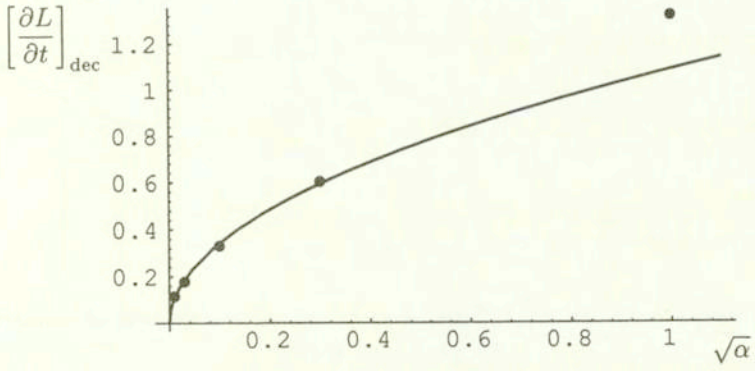

FIG. 8. α-dependence of the decaying term $[\partial L/\partial t]_{\mathrm{dec}}$ in Vinen equation (Schwarz simulation) – dots, and square root α dependence of line reduction after reconnection. The line is fitted to first four points, i.e. for $\alpha < 1$.

2.2. The case $V_{ns} = \text{const} \neq 0$

The absolute value of coefficient α' is smaller than α and unity, and the preliminary simulations show that the last term of Eq. (1.9) does not play any significant role in the vortex line evolution. In further analysis, for the sake of simplicity, we put $\alpha' = 0$.

In the superfluid reference frame with $v_{ns} = \text{const} \neq 0$, $\alpha' = 0$, Eq. (1.9) reads

$$\dot{s} = s' \times s'' + \alpha s'' + \alpha s' \times v_{ns} \,. \tag{2.18}$$

According to the scaling properties of the above equation for each configuration, the characteristic dimension D and also the line-length change Δl are given by some functions f, g.

$$D = \frac{\mathrm{f}(\tau * v_{ns}^2, \alpha, \varphi)}{v_{ns}} \,, \tag{2.19}$$

$$\Delta l = \frac{\mathrm{g}(\tau * v_{ns}^2, \alpha, \varphi)}{v_{ns}} \,. \tag{2.20}$$

The quantity $\tau * v_{ns}^2$ plays the role of an effective time.

Immediately after the reconnection, when the characteristic curvature is large, the vortex line evolution is dominated by the first 2 terms of Eq. (2.18). After some time, when the characteristic curvature gets smaller, the last term dominates the motion of a vortex.

We consider 6 characteristic configurations (Fig. 9).

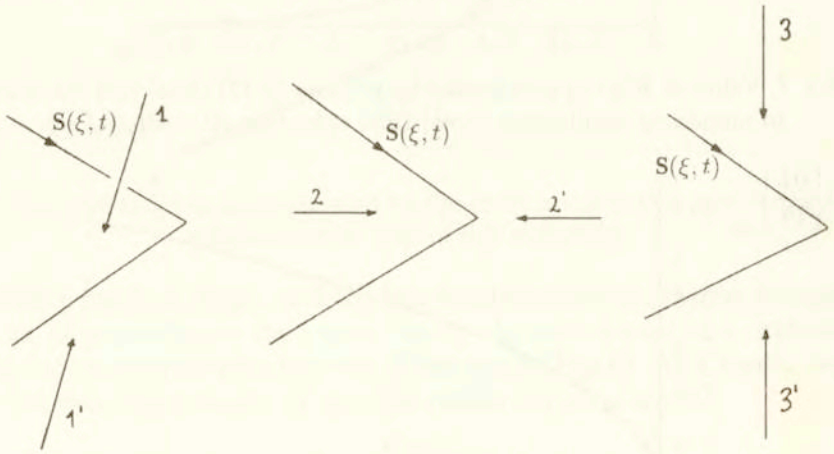

FIG. 9. Six characteristic configurations. Arrows show the direction of counterflow velocity for each configuration.

In the configuration 1 and 1′ the counterflow velocity is perpendicular to the initial vortex plane. In the first case, component $\alpha s' \times v_{ns}$ of the vortex velocity

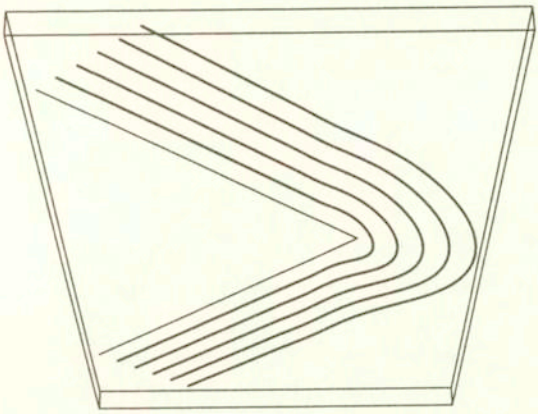

FIG. 10. The vortex evolution in configuration 1 (counterflow velocity perpendicular to the initial vortex plane).

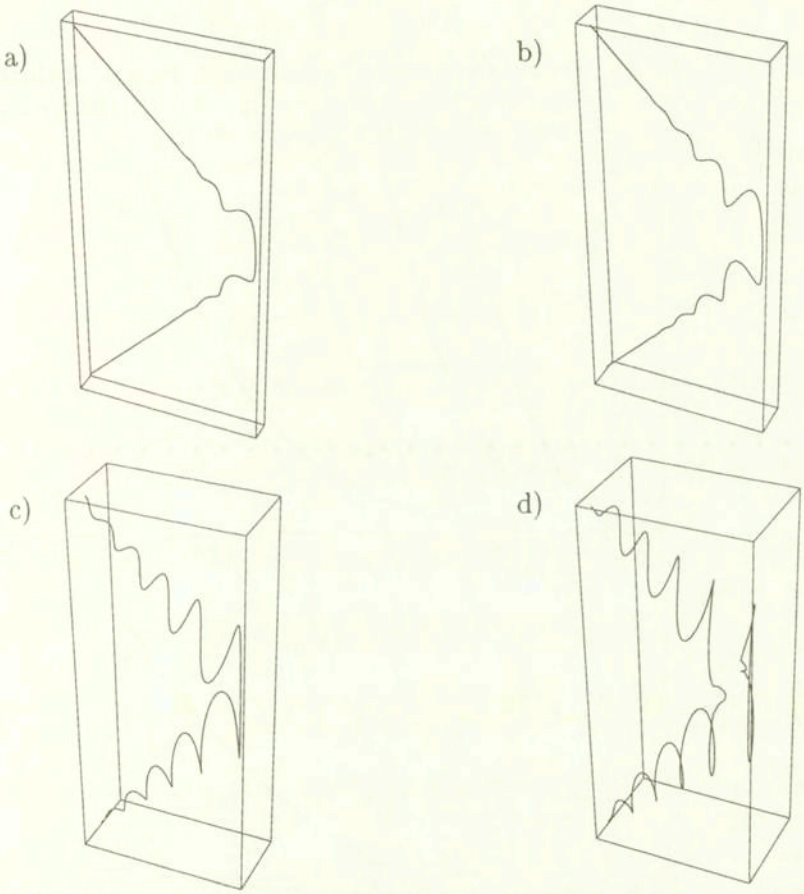

FIG. 11. The vortex evolution in configuration 2 for $\alpha = 0.3$, a) $\tau * v_{ns}^2 = 32$, b) $\tau * v_{ns}^2 = 64$, c) $\tau * v_{ns}^2 = 96$, d) $\tau * v_{ns}^2 = 128$. The separated vortex ring is seen at the bottom.

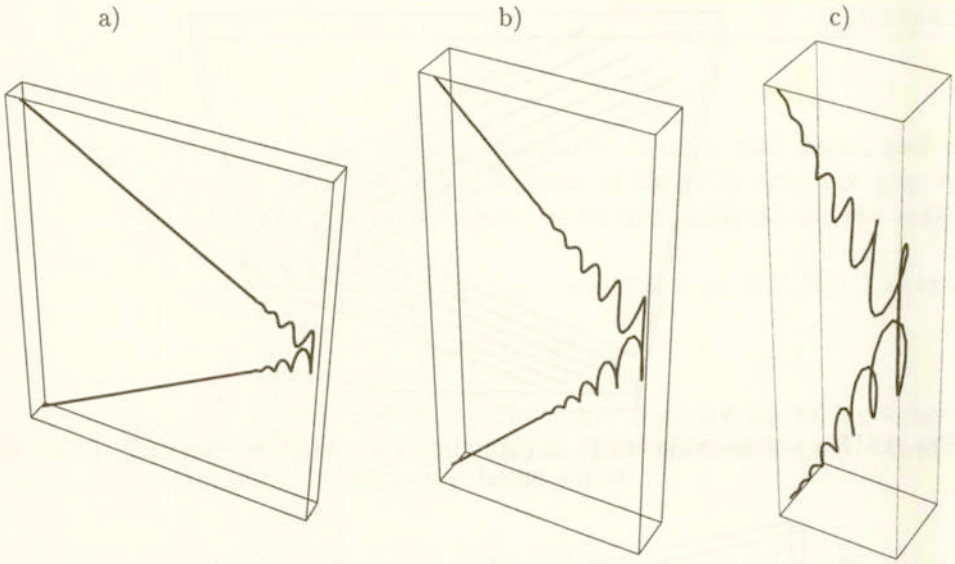

FIG. 12. The vortex line just before reconnection in configuration 2 for three different reconnection angles. The vortex ring separates at $\tau * v_{ns}^2 = 57, 79, 198$ for reconnection angles 30°, 45°, 60°, respectively.

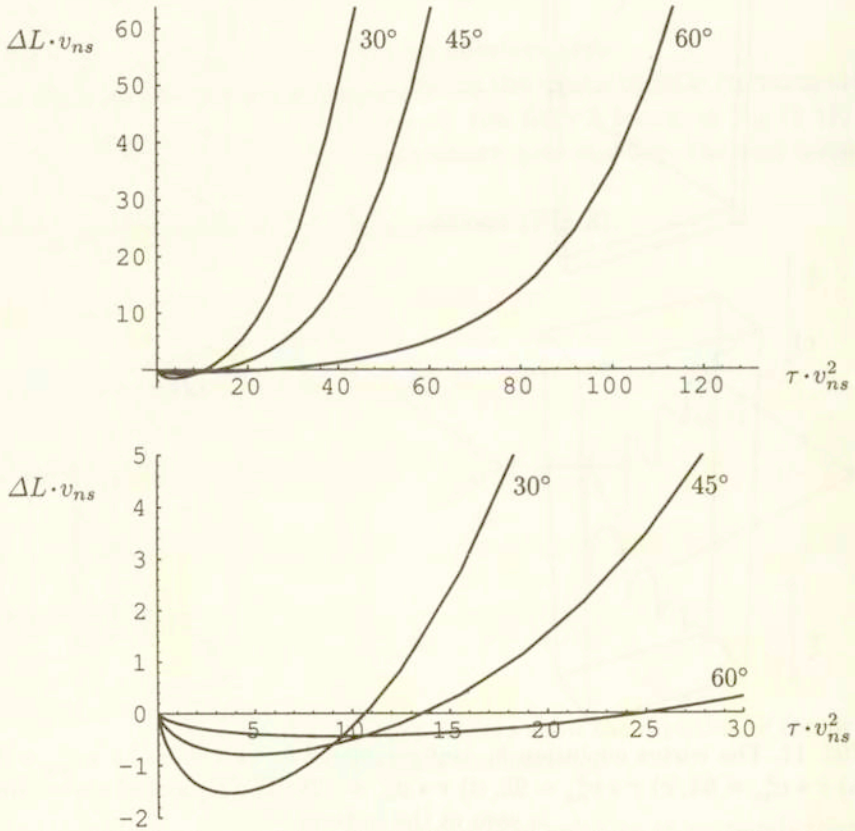

FIG. 13. Line-length changes in configuration 2 for 3 various reconnection angles 30°, 45°, 60°. Lower figure – the same functions for small $\tau * v_{ns}^2$.

is directed outwards and the vortex lengthens (Fig. 10), while in configuration $1'$ the vortex line shortens.

The vortex evolution in configurations $2, 2', 3, 3'$ is much more interesting. The magnitude of component $\alpha s' \times v_{ns}$ of the vortex velocity depends on the relative angle between the direction of the counterflow, and the local tangent to the vortex, and so it varies along the vortex line. As a result, some parts of the vortex line move faster than the others – this starts the vortex loop formation.

In the configurations 2 and $2'$ the counterflow velocity lies in the initial vortex plane and is parallel to the axis of symmetry. The self-induced velocity directs the vertex above the initial vortex plane. If the velocity component $\alpha s' \times v_{ns}$ is also (initially) directed above that plane (configuration 2), the loops form easily. After the loops are formed, the vortex reconnects with itself and vortex ring separates (Fig. 11). The time of ring separation increases with growing reconnnection angle φ (Fig. 12). Figure 13 illustrates the time dependence of total line length (with separated ring) of the vortex. Immediately after the reconnection, as we can

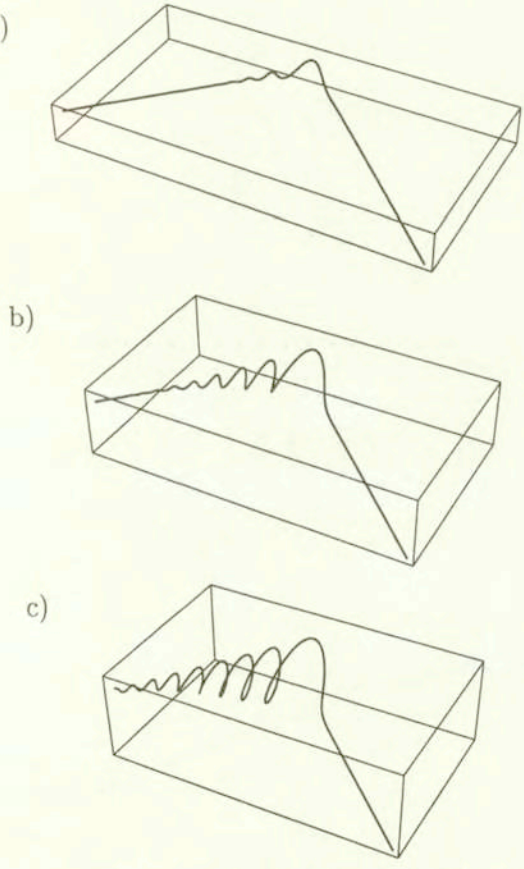

FIG. 14. The vortex evolution in configuration 3. $\alpha = 0.3$, a) $\tau * v_{ns}^2 = 50$, b) $\tau * v_{ns}^2 = 104$, c) $\tau * v_{ns}^2 = 144$.

expect from the previous section, the vortex line shortens (Fig. 13b), but for longer times the line-length increases. The smaller is the reconnection angle, the faster increases the line length (Fig. 13a).

The configurations 3 and 3′ are symmetrical each to other. The instability propagates from the vertex of the filament onto one of angle arms on which loops are formed (Fig. 14). Even for reconnection angles φ close to $\pi/2$, the instability produces the cascade of loops (Fig. 15). For reconnection angles close to $\pi/2$, the loops lie (roughly speaking) on a cone with axis parallel to v_{ns}. The $\alpha s' \times v_{ns}$ velocity component directed outwards the cone increases the loops. Because of this mechanism, the lines parallel to counterflow velocity are very unstable, even a small kink on a line can initiate the cascade of loops. The line-length changes are growing with the growing reconnection angle up to the angle of roughly 60°, and then get smaller for larger angles (Fig. 16). The last result is due to the fact that for reconnection angles closer to $\pi/2$, longer time is needed to initiate the cascade of loops.

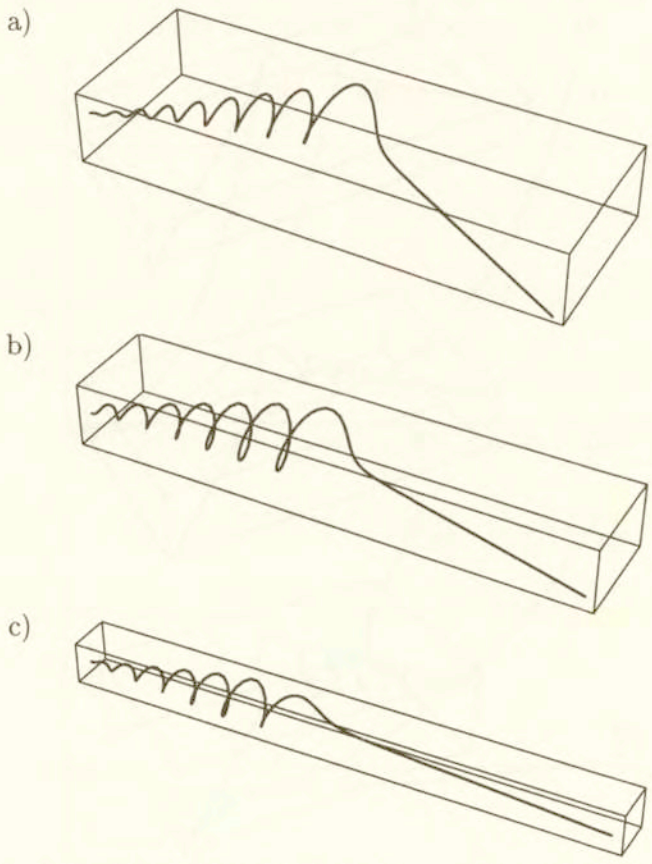

FIG. 15. Loops generation after reconnnection in configuration 3 for 3 different reconnection angles: a) $\varphi = 60°$, b) $\varphi = 75°$, c) $\varphi = 85°$ for $\alpha = 0.3$, $\tau * v_{ns}^2 = 81$.

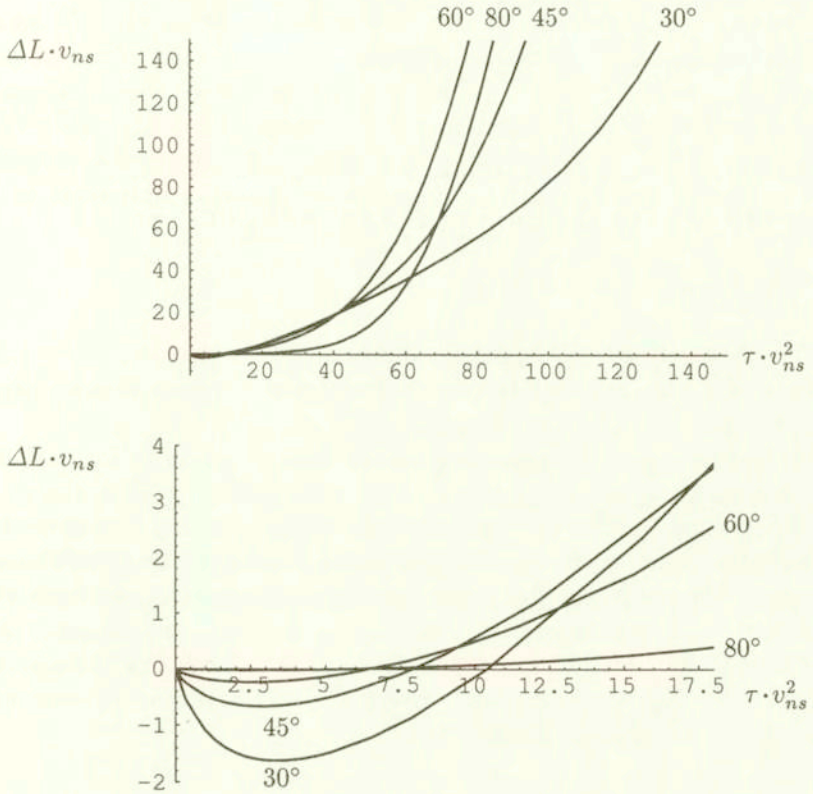

FIG. 16. Line-length changes in configuration 3 for 4 different reconnection angles: 30°, 45°, 60°, 80°. Lower figure – the same functions for small $\tau * v_{ns}^2$.

3. Conclusion

Equation (2.16), confirmed by numerical simulations, describing the line reduction $\Delta l(\alpha, \varphi, \tau)$ is the main result of the first part of the paper. Besides, we found that

$$\int |s''|^2 d\xi = \frac{B}{2\sqrt{\alpha\tau}}, \tag{3.1}$$

with B given by Eq. (2.17) with a resonable accuracy.

To interpret the main result of the first part, let us recall the Vinen equation with Schwarz coefficients

$$\frac{\partial L}{\partial \tau} = \alpha I_l V_{ns} L^{3/2} - \alpha c_2^2 L^2, \tag{3.2}$$

where is $I_l(\alpha)$ an anisotropy coefficient, and

$$c_2^2(\alpha) = \frac{\langle |s''|^2 \rangle}{L} \tag{3.3}$$

measures the average curvature of the vortex tangle. SCHWARZ [6] measured I_l and c_2^2 in numerical simulations performed for 5 various values of α. Now assume that the reconnection rate does not depend on α which seems to be resonable, at least for $\alpha \ll 1$, when vortex dynamics is dominated by the first term in Eq. (2.1). If so, the dependence of the line-length reduction on $\sqrt{\alpha}$ after reconnection should correspond to α dependence of the second term in Vinen equation describing decay of the vortex tangle. Namely

$$c_2^2 \alpha = C\sqrt{\alpha}. \tag{3.4}$$

The best fit (shown in Fig. 7) to four points (with $\alpha < 1$) gives $C = 1.1$. The good fit (for $\alpha < 1$) assures that the line reduction after reconnections plays the key role in decaying of the vortex tangle.

In the second part we have presented the mechanism of loops formation initiated by a reconnection, which probably plays an important role in rise of quantum turbulence when spacing beetwen vortices is relatively big. In a dense tangle, the reconnections occur so frequently that time of undisturbed evolution after each reconnection is too short for loops formation. As one can see from Figures 13 and 16, there is a characteristic time (t_0 for a given configuration and reconnection angle) for which the net growth is equal to zero. For the equlibrium density, the characteristic time spacing between vortex segments reconnection should correspond to average value of t_0.

Acknowledgments

This work was supported by the KBN grant 7T07A03412.

References

1. L. LANDAU, J. Phys., **5**, 71, 1941.
2. L. ONSAGER, Nouovo Cimento, **6**, 249, 1949.
3. R.P. FEYNMAN, [in:] Progress in Low Temperature Physics, Vol. I, p. 17, C.J. GORTER [Ed.], North-Holladnd, Amsterdam 1955.
4. W.F. VINEN, Proc. R. Soc. London, **A 240**, 114, (**240**, 128), (**242**, 493), 1957.
5. K.W. SCHWARZ, Phys. Rev., **B 31**, 5782, 1984.
6. K.W. SCHWARZ, Phys. Rev., **B 38**, 2398, 1988.

POLISH ACADEMY OF SCIENCES
INSTITUTE OF FUNDAMENTAL TECHNOLOGICAL RESEARCH
e-mail: tlipnia@ippt.gov.pl

Received November 7, 1997.